Supporting Information for "Regional Structure of the Polar Vortex via Planetary Wave Phase Diagnostics and Its Link to Cold Air Outbreaks"

Varunesh Chandra[1,2*], Muyin Wang[1,2], James E. Overland[1]

[1] NOAA/Pacific Marine Environmental Laboratory, Seattle WA, USA

[2] Cooperative Institute for Climate, Ocean and Ecosystems Studies, University of Washington, Seattle WA, USA

*Corresponding Author: varunesh@uw.edu

Revised for npj Climate and Atmospheric Science

April 2026

Contents

Eq. S1: Wave activity flux

$$W = \frac{p\cos\varphi}{2|U|}\cdot\begin{cases}\frac{U}{a^2\cos^2\varphi}[(\frac{\partial\psi'}{\partial\lambda})^2 - \psi'\frac{\partial^2\psi'}{\partial\lambda^2}] + \frac{V}{a^2\cos\varphi}[(\frac{\partial\psi'}{\partial\lambda}\frac{\partial\psi'}{\partial\varphi}) - \psi'\frac{\partial^2\psi'}{\partial\lambda\partial\varphi}] \\ \frac{U}{a^2\cos\varphi}[(\frac{\partial\psi'}{\partial\lambda}\frac{\partial\psi'}{\partial\varphi}) - \psi'\frac{\partial^2\psi'}{\partial\lambda\partial\varphi}] + \frac{V}{a^2}[(\frac{\partial\psi'}{\partial\varphi})^2 - \psi'\frac{\partial^2\psi'}{\partial\varphi^2}]\end{cases}$$

In this formulation, $|U|$ represents the climatological mean magnitude of the wind. In the expression, U and V denote the zonal and meridional wind components, respectively, while ψ is the stream function. The variable p is normalized pressure. The parameters a, λ, and φ correspond to the Earth's radius, longitude, and latitude, respectively. A prime symbol (′) indicates an anomaly relative to the climatological mean.

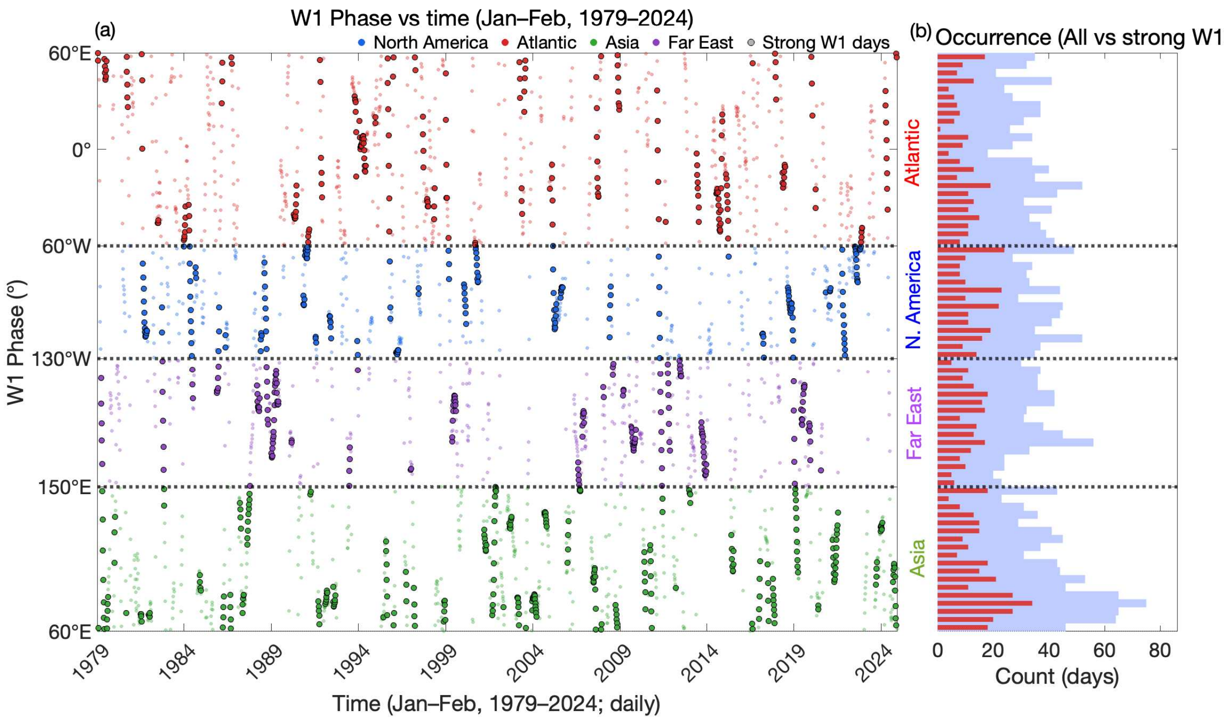

Fig. S1| Temporal distribution and occurrence frequency of W1 trough phases (1979–2024). (a) Daily W1 phase color-coded by sector. (b) Sector-wise occurrence histograms for all days (blue) and strong-W1 days (red).

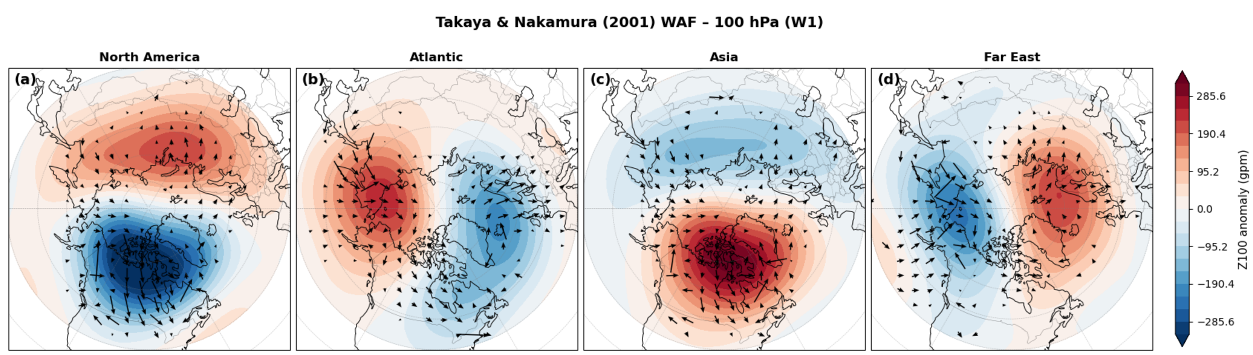

Fig. S2| Takaya and Nakamura (2001) horizontal wave-activity flux (WAF) at 100 hPa during strong Wave-1 (W1) events. Shading shows Z100 geopotential height anomalies, and vectors indicate the horizontal WAF, illustrating the propagation of planetary-wave activity toward the polar vortex trough. Composites are computed using ERA5 daily geopotential height fields for January–February from 1979 to 2024.

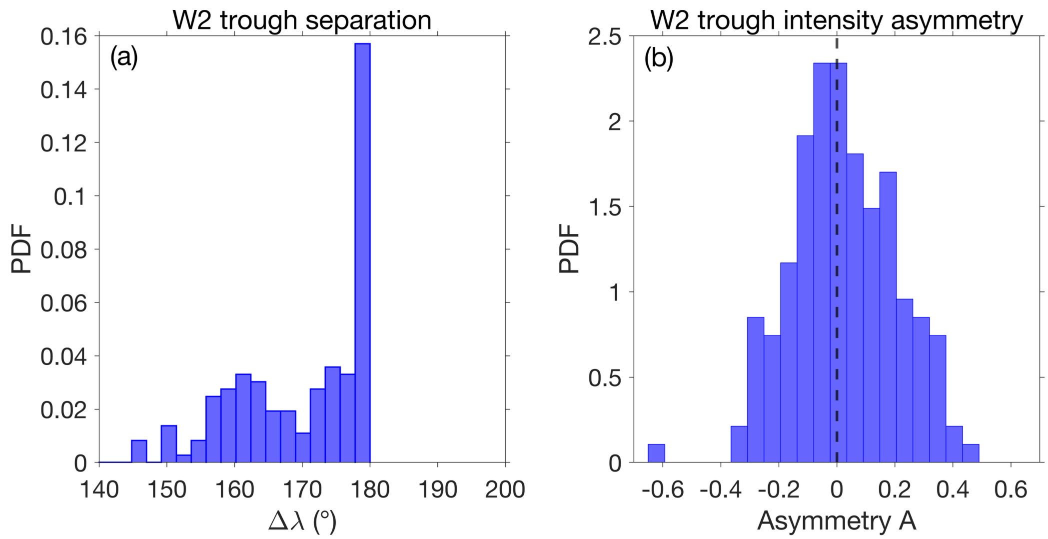

Fig. S3| Geometric properties of the Wave-2 structure at 100 hPa. Left (a): Distribution of angular separation $\Delta\lambda$ between the two W2 troughs identified from observed anomaly minima near the phase-predicted lobe locations. The separation is typically close to opposite in longitude (mean ≈170°, 95% CI: 148–180°), consistent with a wave-2 geometry but allowing substantial variability across events. Right (b): Distribution of trough intensity asymmetry A, showing that the relative strength of the two lobes varies widely, so one lobe frequently dominates. This variability in lobe intensity helps explain the sector-dependent patterns discussed in Figure 5.

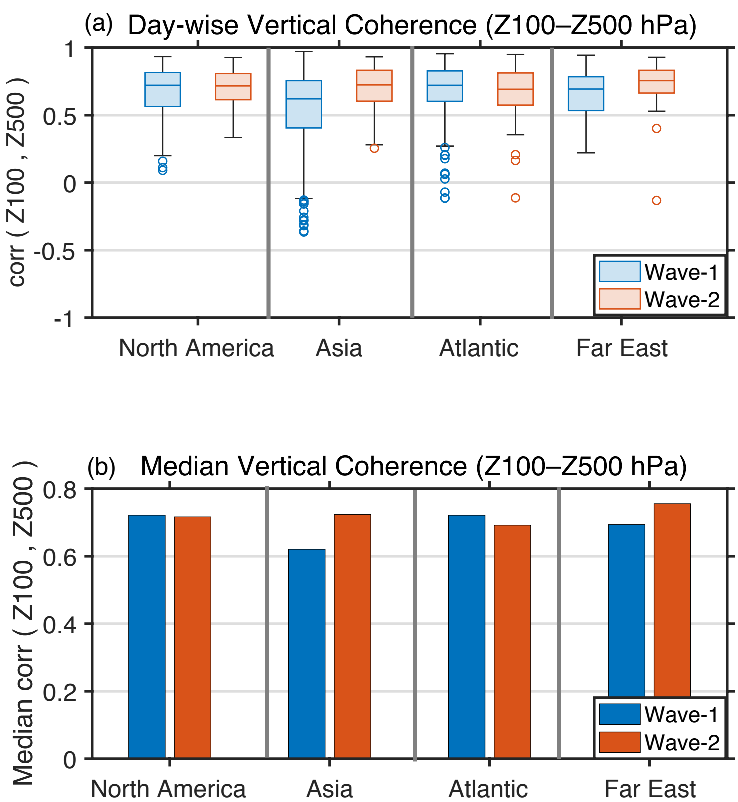

Fig. S4| Vertical coherence between lower-stratospheric (100 hPa) and mid-tropospheric (500 hPa) geopotential height anomalies. (a) Day-wise correlations for all strong W1 and W2 events. (b) Sector-wise medians. Both wave types exhibit robust vertical connections.

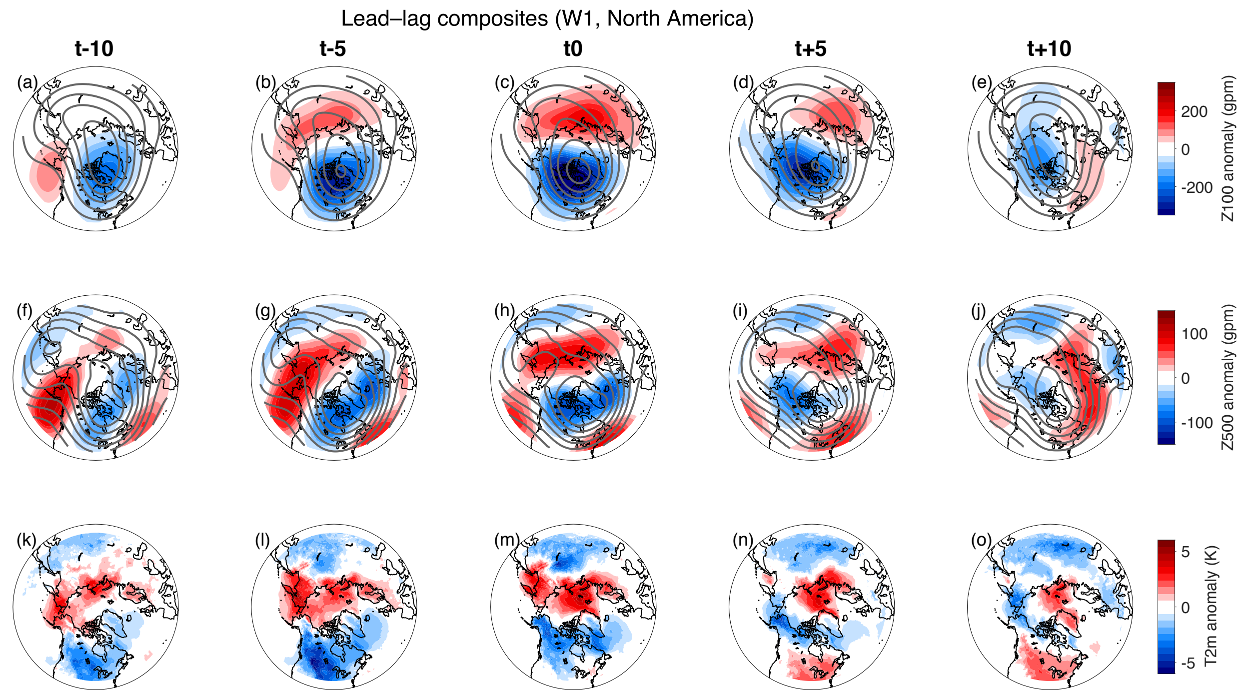

Fig. S5| Lead–lag evolution of Wave-1 trough events over the North America sector (t−10 to t+10 days). Each column represents a different lag day relative to the t0 W1 trough, progressing from 10 days before (t−10) to 10 days after (t+10). The top row shows 100-hPa geopotential height anomalies (shading) with raw contours, while the middle row displays 500-hPa geopotential height anomalies (shading) with corresponding raw contours. The bottom row presents 2-meter temperature (T2m) anomalies.

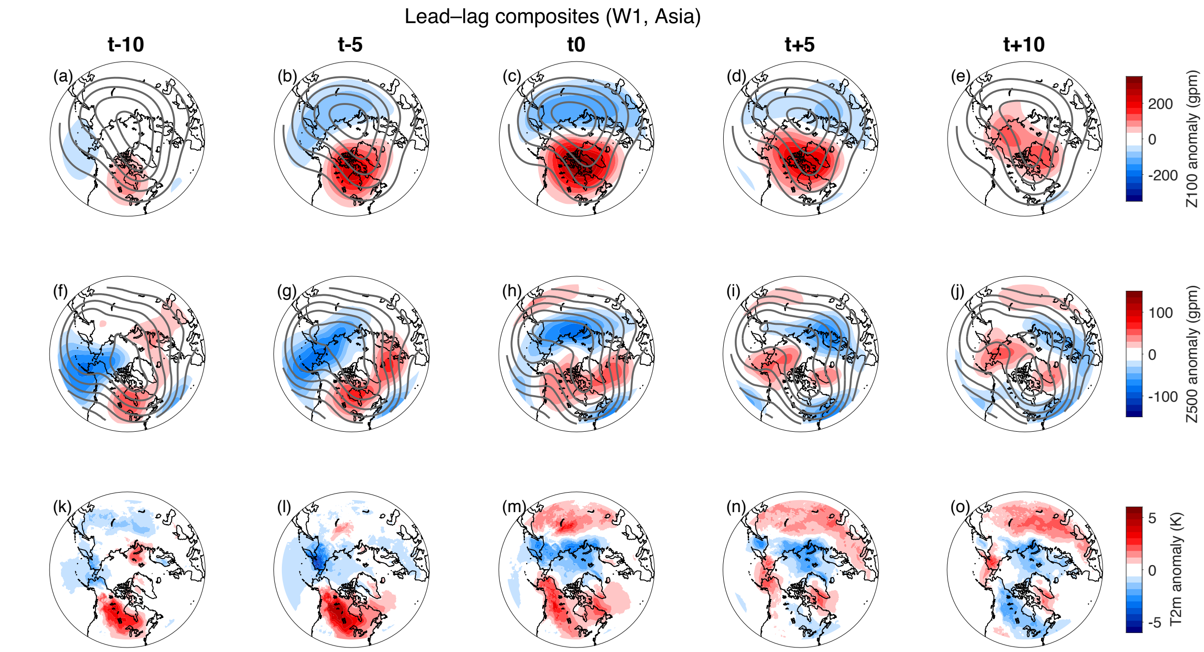

Fig. S6| Lead–lag evolution of Wave-1 trough events over the Asia sector (t−10 to t+10 days). Each column represents a different lag day relative to the t0 W1 trough, progressing from 10 days before (t−10) to 10 days after (t+10). The top row shows 100-hPa geopotential height anomalies (shading) with raw contours, while the middle row displays 500-hPa geopotential height anomalies (shading) with corresponding raw contours. The bottom row presents 2-meter temperature (T2m) anomalies.

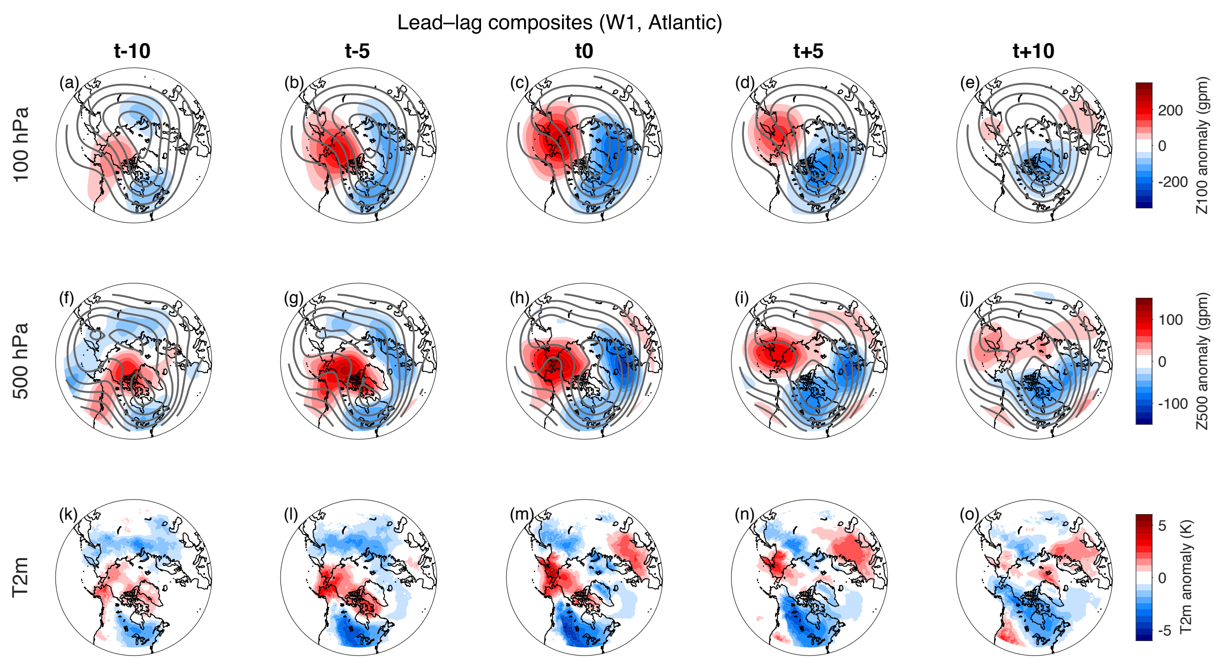

Fig. S7| Lead–lag evolution of Wave-1 trough events over the Atlantic sector (t−10 to t+10 days). Each column represents a different lag day relative to the t0 W1 trough, progressing from 10 days before (t−10) to 10 days after (t+10). The top row shows 100-hPa geopotential height anomalies (shading) with raw contours, while the middle row displays 500-hPa geopotential height anomalies (shading) with corresponding raw contours. The bottom row presents 2-meter temperature (T2m) anomalies.

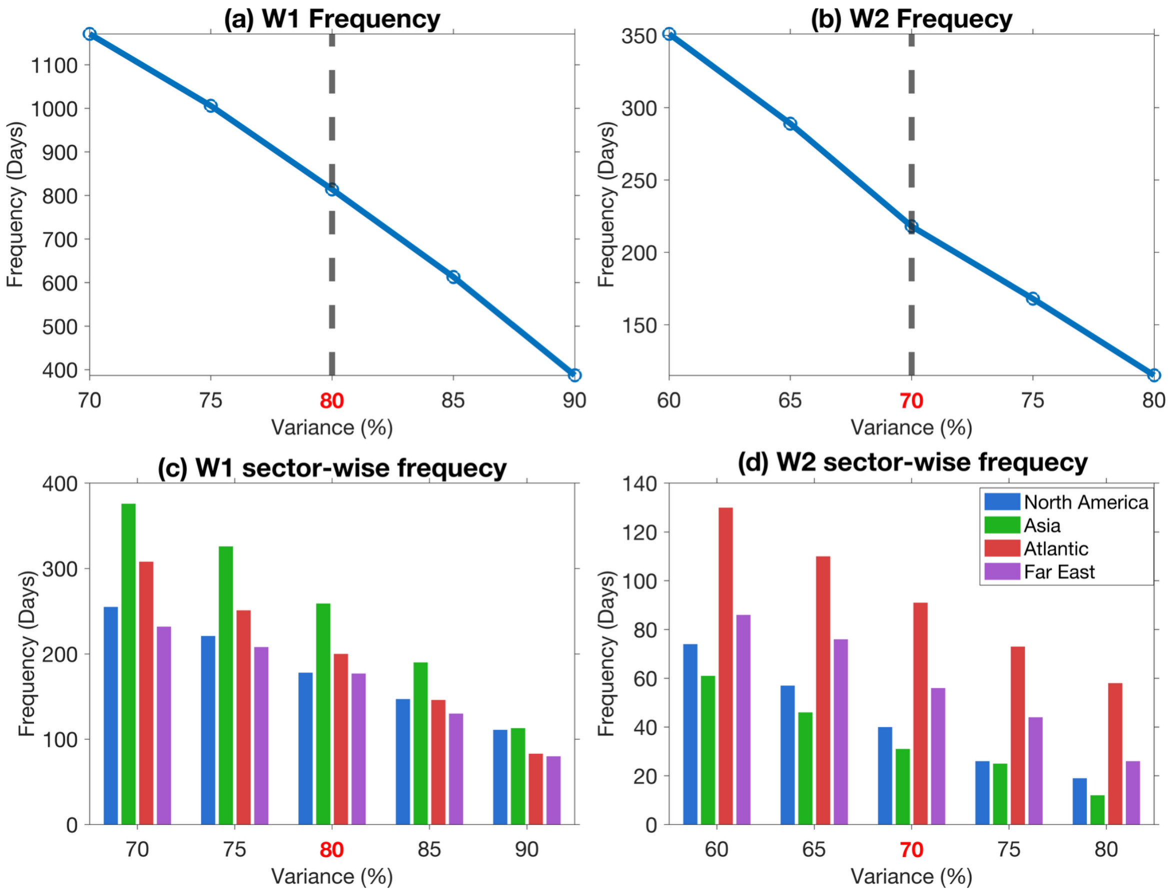

Fig. S8 | Sensitivity of strong-wave identification to variance (%) thresholds. (a,b) Total number of strong W1 and W2 days as a function of the longitudinal spatial variance (%) explained by each harmonic. Vertical dashed lines indicate the baseline thresholds used in the main analysis (W1 ≥ 80% variance; W2 ≥ 70% variance; see Methods for definition). (c,d) Sector-wise frequency of strong-wave days under varying thresholds. Although the absolute number of events decreases as the threshold increases, the four anchoring regions and their relative frequency structure remain stable across ±5–10 percentage-point perturbations of the variance threshold, indicating robustness of the geometric classification.

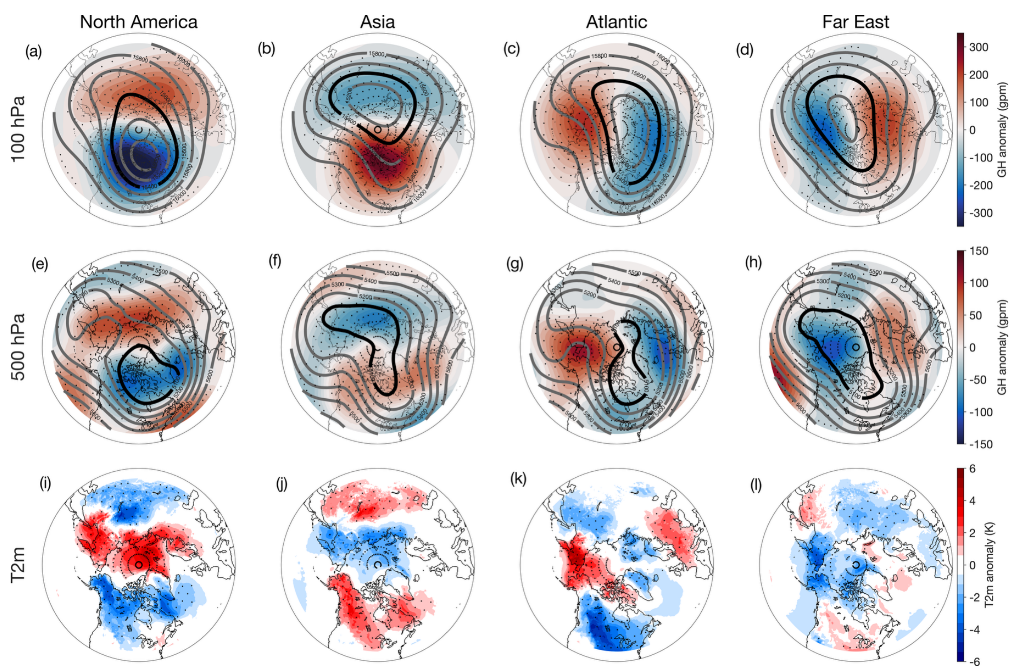

Fig. S9 | Statistical significance of W1 composite anomalies shown in Fig. 4. Stippling indicates regions where the composite anomalies are statistically significant at the 95% confidence level based on a two-sided Student's t-test. Panel layout follows Fig. 4: top row (a–d) 100-hPa geopotential height anomalies, middle row (e–h) 500-hPa geopotential height anomalies, and bottom row (i–l) 2-m temperature anomalies across the four sectors (North America, Asia, Atlantic, Far East).

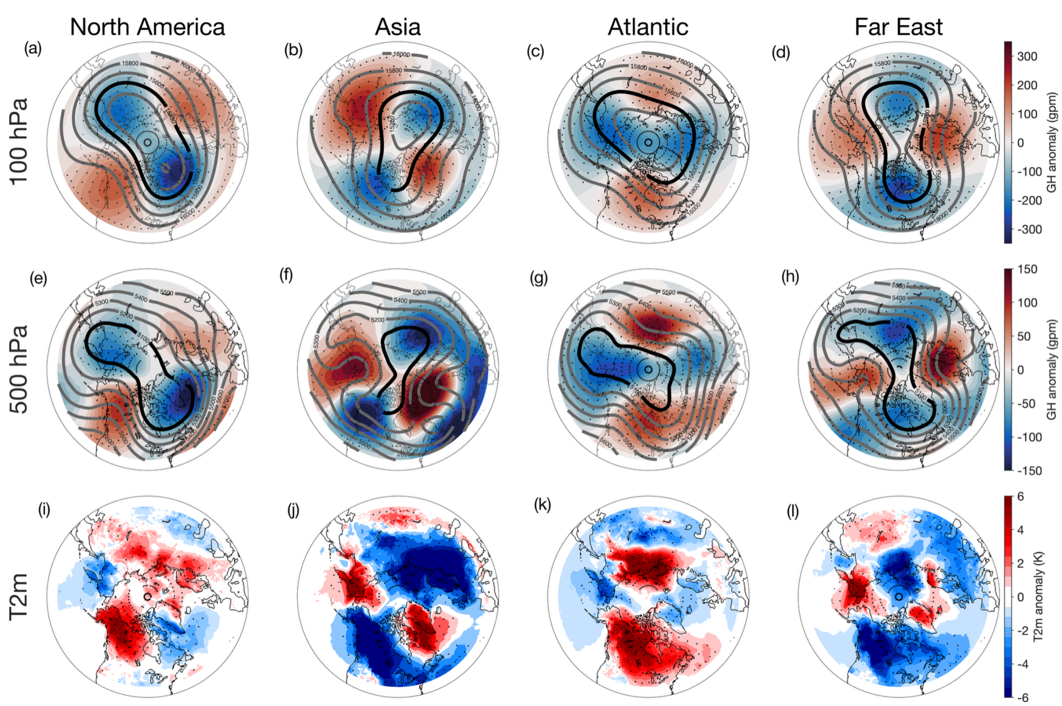

Fig. S10 | Statistical significance of W2 composite anomalies shown in Fig. 5. Stippling indicates regions where the composite anomalies are statistically significant at the 95% confidence level based on a two-sided Student's t-test. Panel layout follows Fig. 5: top row (a–d) 100-hPa geopotential height anomalies, middle row (e–h) 500-hPa geopotential height anomalies, and bottom row (i–l) 2-m temperature anomalies across the four sectors (North America, Asia, Atlantic, Far East).